



**HAL**  
open science

## An automatized frequency analysis for vine plot detection and delineation in remote sensing

Carole Delenne, Gilles Rabatel, M. Deshayes

► **To cite this version:**

Carole Delenne, Gilles Rabatel, M. Deshayes. An automatized frequency analysis for vine plot detection and delineation in remote sensing. *IEEE Geoscience and Remote Sensing Letters*, 2008, 5 (3), p. 341 - p. 345. 10.1109/LGRS.2008.916065 . hal-00454439

**HAL Id: hal-00454439**

**<https://hal.science/hal-00454439>**

Submitted on 8 Feb 2010

**HAL** is a multi-disciplinary open access archive for the deposit and dissemination of scientific research documents, whether they are published or not. The documents may come from teaching and research institutions in France or abroad, or from public or private research centers.

L'archive ouverte pluridisciplinaire **HAL**, est destinée au dépôt et à la diffusion de documents scientifiques de niveau recherche, publiés ou non, émanant des établissements d'enseignement et de recherche français ou étrangers, des laboratoires publics ou privés.

# An automatized frequency analysis for vine plot detection and delineation in remote sensing

Carole Delenne, Gilles Rabatel and Michel Deshayes

**Abstract**—The availability of an automatic tool for vine plot detection, delineation and characterization would be very useful for management purposes. An automatic and recursive process using frequency analysis (with Fourier Transform and Gabor filters) has been developed to meet this need. This results in the determination of vine plot boundaries determination and accurate estimation of inter-row width and row orientation. To foster large-scale applications, tests and validation have been carried out on standard very high spatial resolution remotely sensed data. About 89% of vine plots are detected corresponding to more than 84% of vineyard area and 64% have correct boundaries. Compared to precise on-screen measurements, vine row orientation and inter-row width are estimated with an accuracy of respectively 1° and 3.3 cm.

**Index Terms**—Remote-sensing, vineyard, detection, segmentation, frequency analysis, Gabor filters.

## I. INTRODUCTION

THE increasing availability of very high spatial resolution (VHSR) aerial images offers a lot of new potential applications as the shape or the spatial structure of observed objects is more distinguishable. In the agricultural domain, for instance, various types of vegetation can be distinguished according to their spatial patterns (cereal crops, forests, orchards, etc.). However, because they deal with spatial structures or shapes, these applications require new image processing approaches, even if multispectral aspects remain important (e.g. as a preliminary tool to enhance the image contrast). Several shape-model based approaches can thus be found in the literature, especially for building detection [1], [2] or isolated trees detection [3]. For forest identification, various textural approaches based on co-occurrence matrices are proposed [4], [5]. Most vineyard related studies using remote-sensed data aim to characterize already delineated plots e.g. by detecting vine rows [6] or by characterizing training mode [7] or foliar density [8]. A very important feature in vineyard is the spatial periodicity of the crop pattern, due to the training system (often in rows or grid), which is clearly visible in VHSR aerial images. A vineyard can thus roughly be approximated to a local planar wave of a given spatial frequency and orientation. Therefore, approaches based on spatial frequency analysis, and notably on the Fourier spectrum, are particularly suited. Wassenaar et al. [7] showed the ability of such an approach to characterize vine plots (orientation, inter-row width, training system). In [9] and [10], the authors attempted to detect vine plots with a method based on the wavelet transform. However, this method is not satisfactory for mainly three reasons: 1) it needs a significant user intervention because the filtering scheme is not selective enough, 2) results are obtained as pixel

classification (plots boundaries are not provided), and 3) using a plot basis validation, only 78% of plots were accurately classified. In [11], periodical vineyard patterns are detected by computing and analyzing the grey-level autocorrelation function along four predefined directions in the image. This approach can be compared in many points to a frequency analysis<sup>1</sup>. However, although providing good results on American vineyards, this could not be successfully applied on old European vineyard regions as only four frequency orientations are considered. In [12], a frequency analysis using Gabor filters is proposed in a study concerning olive tree plots; but these filters were manually determined from the observation of the Fourier spectrum. These approaches aiming at vine plot detection only provide a vine/non-vine pixel classification without the determination of plot boundaries. In a recent study, Da Costa et al. [13] applied a textural approach to meet this need. Even if the results obtained on several plots (less than 10) are good, it seems difficult to generalize this method as it is applied on a 0.15 cm resolution and needs the user to select a window inside the field he wants to process. Moreover, a previous comparative study for vine plot detection [14] showed the superiority of a frequency analysis on a such textural approach (also based on a difference between cooccurrence features calculated along two perpendicular directions).

A basic issue of vine plot detection and delineation in VHSR images can be highlighted: on the one side, periodical patterns have very specific and clearly defined properties that should allow their detection; but on the other side, the large range of possible orientations and inter-row widths that have to be considered in a detection process prevents from using classical textural approaches. We thus propose an original scheme that overcomes this paradox, by using an automatic setting of Gabor filters through a recursive process (of which a first implementation was presented in [15]).

The aim of this letter is to present the theoretical aspects, as well as the recursive implementation of the operational algorithm developed for the automatic vineyard *detection, delineation* and *characterization* on very large aerial images for inventory and management purposes<sup>2</sup>. Then, only first results obtained on a standard VHSR image<sup>3</sup>, in natural colors and with a 50 cm resolution, are given. Further work will be done to analyze the effect of the image characteristics on the results.

<sup>1</sup>The autocorrelation function can be obtained as the inverse Fourier transform of the power spectrum.

<sup>2</sup>See <http://www.bacchus-project.com> for more details.

<sup>3</sup>Such as the Bd-Ortho<sup>®</sup> provided every five years by the French Geographical Institute and covering the whole French territory.

## II. METHOD

## A. Principle

1) *Grey-level image preprocessing*: Frequency analysis deals exclusively with spatial structures without considering their radiometric properties in the image. The proposed algorithm uses grey-level images with the only requirement of a sufficient contrast between vine rows and inter-rows for the parallel structure to be visible. Thus, depending on the spectral bands available, these images can be of various type, *e.g.* one particular spectral band, indexes such as NDVI (Normalised Difference Vegetation Index), luminance computed from a RGB image, or even Digital Surface Model issued from Lidar data. The comparison of these possibilities will not be addressed here. In any case, a normalisation preprocessing is applied to ensure the parameter robustness in the following treatments. It consists in a local linear transformation which normalizes the mean and standard deviation in a sliding window, so that different vineyard structures will generate comparable Fourier amplitude peaks.

2) *Gabor filtering*: Figure 1 shows a typical vineyard image and its Fourier spectrum, on which several pieces of information have been added for better understanding. The amplitude peaks (three of them being circled) observed in the frequency domain correspond to the vineyard plots in the spatial domain. Each position  $(u, v)$  in the Fourier Spectrum represents a particular frequency from  $-0.5$  to  $+0.5$ <sup>4</sup>. Vine rows orientation  $\theta$  in a geographical coordinate system and inter-row width  $w$  are directly linked to this position by:

$$\theta = \cos\left(\frac{u}{\sqrt{u^2 + v^2}}\right), \quad w = \frac{1}{\sqrt{u^2 + v^2}} \quad (1)$$

The main idea of our process is to isolate each individual plot  $i$  by selecting its corresponding frequency  $(u_i, v_i)$  in the Fourier spectrum using a Gabor filter [16]. In the spatial domain, this filter is defined as:

$$h_{u_i, v_i} = g(x, y) \cdot e^{-2\pi j(u_i x + v_i y)} \quad (2)$$

where

$$g(x, y) = \frac{1}{2\pi\sigma^2} \cdot e^{-\frac{x^2 + y^2}{2\sigma^2}} \quad (3)$$

In the frequency domain, the Fourier transform of  $h_{u_i, v_i}$  is a Gaussian function of width  $1/(2\pi\sigma)$  centered on  $(u_i, v_i)$ :

$$H_{u_i, v_i}(u, v) = e^{-2\pi^2\sigma^2((u-u_i)^2 + (v-v_i)^2)} \quad (4)$$

Figure 2 shows three examples of Gabor filtered outputs corresponding to three different amplitude peaks in the original Fourier spectrum. As we can see, this filtering process appears to be very efficient in selecting vine plot areas with a given frequency (*i.e.* a given  $(\theta, w)$  characteristics).

Both for computational reasons and to get exploitable Fourier spectra, this filtering process must be applied on limited size images (typically  $500 \times 500$  pixels). Because studied areas are often much larger, an initial partitioning in square tiles is used. In the following, we only consider the resulting sub-images and will see how to recover plots that have been split by the partitioning.

<sup>4</sup> $\pm 0.5$  corresponds to the highest frequency, *e.g.* the alternation of black and white lines of one pixel widths.

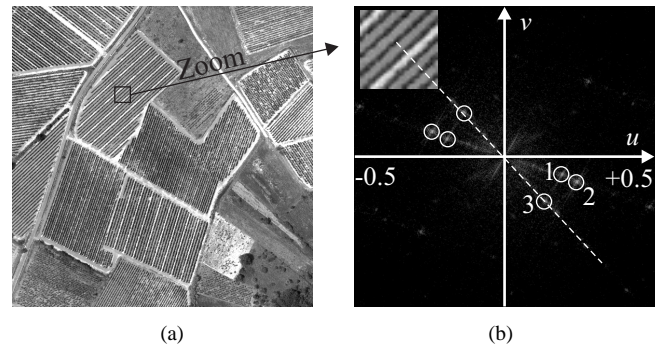


Fig. 1. a) Image (red channel, 50 cm/pixel) of a vineyard area; b) Fourier spectrum (on which several pieces of information have been added).

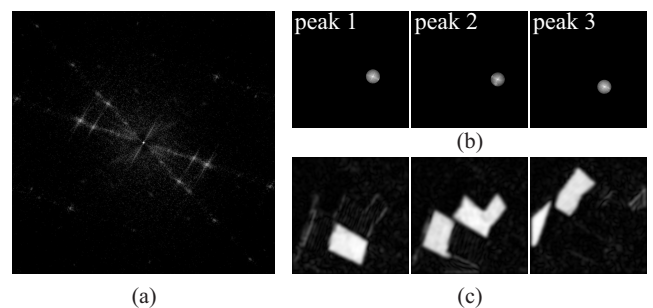


Fig. 2. a) Fourier spectrum; b) Gabor filtering; c) Modulus of the output complex images, *resp.* for peaks 1, 2, 3.

## B. Recursive process

To find out each vine plot in the input image, the Gabor filter has to be applied successively on the amplitude peaks in the Fourier spectrum by adjusting its central frequency  $(u_i, v_i)$ . Due to harmonic frequencies, the same plot can generate several maxima. To overcome this issue, only the highest peak is searched for; when the corresponding plots have been recovered by Gabor filtering, they are listed and erased from the original image by assigning to their pixels a unique value (equal to the image mean in order to avoid the apparition of new frequency peaks). This guarantees that neither the selected peak nor the corresponding harmonics will be selected in further iterations. This process is repeated until no more amplitude peak is found (*i.e.* when the ratio of the maximum and the average amplitude in the Fourier spectrum is lower than a predefined value  $R$ ).

After Gabor filtering, a threshold is applied to the output image. We thus obtain a binary image, in which each object is supposed to be a vine plot with the  $(\theta, w)$  characteristics corresponding to the  $(u_i, v_i)$  center of the current Gabor filter. However, the different plots may not have exactly the same characteristics but very close ones. Some plots may also be incomplete in the current original sub-image if they have been split by the initial partitioning process. For these reasons, each plot is processed again through a new Gabor filter. This is organized as follows:

- A new sub-image is created where all pixels but those of the candidate plot are set to the image mean, so that only its corresponding amplitude peak will appear

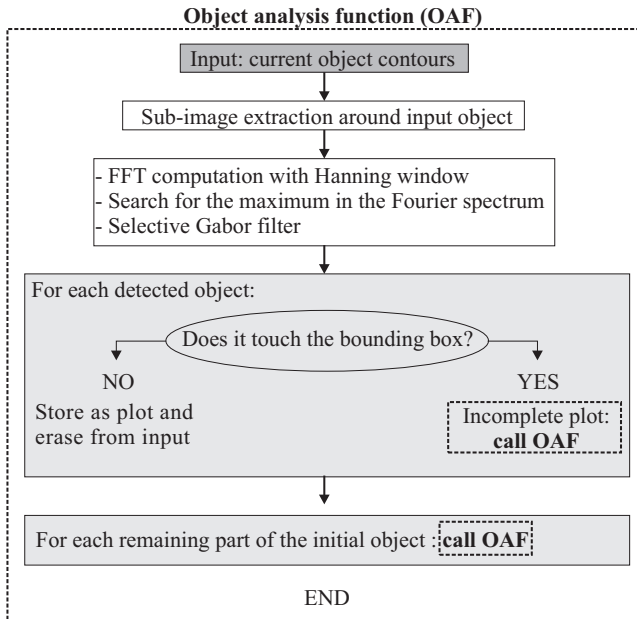


Fig. 3. Summary diagram of the recursive function. Due to recursivity, new OAF call does not mean that the current OAF execution is finished.

in the Fourier spectrum. This guarantees an accurate determination of the plot characteristics  $(\theta, w)$ .

- A new Gabor filter is then applied to the original sub-image around this unique peak. If the resulting binary object extends to the sub-image edge, a new sub-image is built around it, including margins to allow object extension, and the process is repeated. In this way, we are guaranteed to recover the complete plot in one or several iterations.

It appears from these steps that the same filtering and binary analysis scheme is applied many times, starting either from the initial sub-images, or from the current plot candidate, by building a new sub-image around it. The iteration number is not predictable as the sub-image issued from a current binary object can itself generate an undetermined number of new objects. For this reason, a recursive function is particularly suited (figure 3). It is initially applied on ‘virtual’ plots issued from the partitioning. To avoid multiple detections, the already detected vine plots are erased in every new sub-image before further processing. When the whole image has been treated, a GIS layer is generated with the detected plot boundaries. An attribute table is associated to this layer, containing for each plot, its area, row orientation and interrow width.

### III. APPLICATION

#### A. Study area and data acquisition

To assess the global detection process, a study area of 200 ha has been chosen, which is a subset of the La Peyne watershed (110 km<sup>2</sup>) located in the Languedoc-Roussillon region - France. This zone is representative of the French Mediterranean coastal plain with respect to agricultural practices and vineyard management. Despite a general decrease, vine cultivation is still predominant in the study area and concerns about 70% of the Agricultural Area Used.

During the first week of July 2005, a digital camera was used on an U.L.M. (Ultralight motorized) to acquire images in natural colors which have been assembled in an orthophotomosaic of 50 cm spatial resolution. For result validation, the 160 vine and non-vine plots of the site have been manually digitized in a GIS database by photo-interpretation and will be considered as ‘real’ plots (figure 4). Ground-truth information was collected the same day as image acquisition and added in an associated attribute table. This later contains information concerning land use such as vine, orchards, cereal crops and other characteristics for vine plots, such as training mode (e.g. grid, line) or soil surface condition (bare soil or grass covered). Moreover, measurements of  $(\theta, w)$  characteristics have been done by photo-interpretation: mean of 10 measures for row orientation and measure of the longest segment perpendicular to the rows in the plot, divided by the corresponding number of inter-rows, for inter-row width.



Fig. 4. Zoom on the study area and manual vine plot segmentation.

#### B. Process parameters

Four main parameters are used in the process.

A *minimum surface* is set under which no object is considered as a vine plot. A very small value can be taken to ensure the detection, even partial, of most of the plots. In our example, it has been set to half the smallest vine plot of the study area: 200 m<sup>2</sup>. A value of 1 m<sup>2</sup> did not change the results but a too small value could have produced some false detections, on the supposition, however, that their amplitude in the Fourier spectrum is higher than the  $R$  parameter (defined below).

The *Gabor filter width* controls the filter selectivity in the spectral domain and the plot boundaries location accuracy in the spatial domain. Here, the filter width corresponds to 4 m in the spatial domain (*i.e.*  $\sigma = 8$  pixels according to image resolution), which corresponds in the study area to a  $2\sigma$  analysis width containing about 4 vine rows.

The initial image normalization and the Gabor filter selectivity give to vineyard pixels in the output image a very high grey-level value compared to other ones. A simple binary threshold can thus be applied to the filtered output image (see figure 2c). The choice of the *threshold value* is not critical: following results have been obtained with a value of 20 after

renormalization in the 0-255 range, but tests have shown that values until 150 do not change dramatically the results (5 plots are partially detected instead of well-segmented, and the amount of missing plots remains unchanged). Moreover, since the distribution is nearly bimodal, the threshold could also be seek automatically.

In the same way, it has been tested that the *amplitude peak ratio*  $R$  can be chosen in a relatively large range: [15, 25]. Lower values (*e.g.* 10) generate some false plots while greater values (*e.g.* 30) lead to the loss of some badly contrasted plots. Following tests have been carried out with  $R = 20$ .

#### IV. RESULTS AND DISCUSSION

Preliminary tests have shown that the best contrast between vine and soil, even when covered by grass, was obtained with the red channel. Hence, this channel has been directly used thereafter as the input image for the detection algorithm<sup>5</sup>.

To compare our results to those obtained by other studies providing a vine/non-vine pixel classification, we should consider as ‘good classified’, the plots of cases 1, 2, 3, 5 and many plots of the cases 4 and 8 defined below (see table I). This leads to a good classification rate of more than 85 %. However, the aim here is not a pixel classification, but the delineation of vine plots boundaries.

##### A. Segmentation results

The main goal of the developed process is the plot boundaries determination, which has never been proposed before. Therefore, a plot based validation has been performed, comparing automatically and manually segmented plots according to their overlapping rate. Results are given in table I according to eight different cases considered and illustrated in figure 5.

The three most represented types of results are: well segmented plots (64%), under-segmented plots (15.8%) and missing plots (11.4%). Under-segmentation can be considered as good detection as it corresponds to the grouping of neighboring plots that always have the same  $(\theta, w)$ . These plots are usually separated by a narrow road or a ditch but there is sometimes no separation and they only differ by the soil surface condition between rows or by some characteristics undistinguishable in aerial images such as age or height (figure 6(a) down). This kind of segmentation error is inherent to any segmentation method relying on spatial pattern detection: to detect patterns a minimal neighborhood is required. For this reason, we do believe that a further step (presently under development) based on individual vine row analysis is necessary and probably sufficient to overcome this issue.

The undetected plot ratio is relatively weak (11.4%) and mainly concerns small plots, with very few rows, which thus lead to a weak amplitude peak in the Fourier spectrum. Indeed, nine out of the 13 missing plots are smaller than 0.2ha. Consequently, they represent less than 5% of the total vineyard area. Within the four other non-detected plots, one has most of its vine-trees missing (figure 6(b) up), another has a narrow

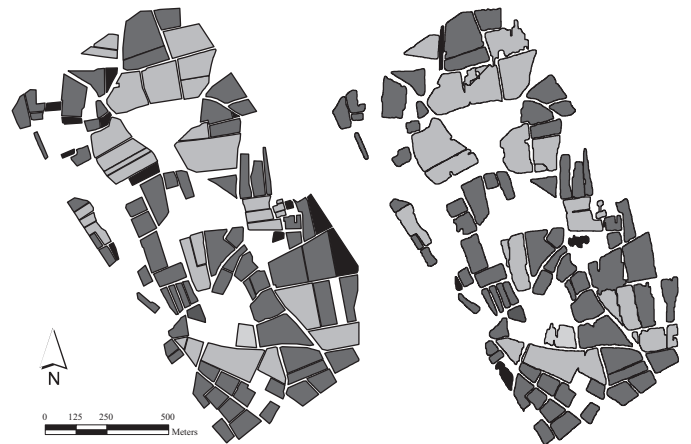


Fig. 5. Comparison of manual (left) and automatic (right) segmentation. In black: non detected plots (left) and false detection (right); in dark grey: good delineation; in light grey: good detection but incorrect delineation.

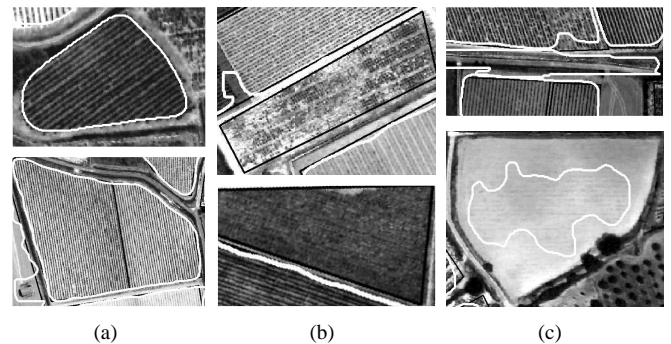


Fig. 6. Result examples. a. good detections (correct and under segmentation); b. not detected vines; c. non-vines segmented as vine plots (manual segmentation in black and automatic in white).

inter-row width (1.7m), close to the detection limit (according to the image resolution), and the two others are very poorly contrasted in the image (figure 6(b) down).

Only four ‘plots’ have been wrongly segmented. One around a longitudinal high grey-level transition (due to a road and its side ditches), which has generated amplitude peaks in the search range (figure 6(c) up). The others are located in non-cultivated plots, but which have been recently ploughed (figure 6(c) down) and therefore present a parallel structure. These ‘plots’ will however easily be eliminated in the further step of vine rows analysis using radiometric criteria.

##### B. Characterization results

Concerning crop pattern characterization, the amplitude peak location in the Fourier spectrum enables the accurate estimation of vine row orientation and inter-row width. Indeed, between on-screen measurements and method estimation, an average absolute difference of less than  $1^\circ$  (respectively 3.3 cm) was found for  $\theta$  (respectively  $w$ ). In addition to the utility of characterization as such, these estimations are needed to extract each vine row for the further step of row analysis<sup>6</sup>.

<sup>5</sup>A detailed analysis of image characteristics influence on the results will be presented in a further paper.

<sup>6</sup>Moreover, it appears in this step that the less accurate method is not the automatic one but the photo-interpretation.

TABLE I  
RESULTS IN NUMBER OF PLOTS AND PERCENTAGE, ACCORDING TO DIFFERENT SEGMENTATION CONFIGURATIONS.

Segmentation types and definitions	Real plots (except for 7)
<b>1. Good:</b> overlapping surface is higher than 70%	72 64 %
<b>2. Over:</b> one real plot is segmented in several plots	2 1.8 %
<b>3. Under:</b> one segmented plot includes several real plots	18 15.8 %
<b>4. Partial:</b> only a part of the plot is detected	0 0 %
<b>5. Larger:</b> the segmented plot overflows onto other plots	5 5.2 %
<b>6. Undetected:</b> not detected vine plots	15 11.4 %
<b>7. False detection:</b> non-vine plots automatically segmented as vine	4
<b>8. Other:</b> Other cases	2 1.8 %

V. CONCLUSION

The proposed automatic and recursive process has proved its efficiency for vineyard detection, delineation and characterization in many ways. While most of detection studies - not only concerning vineyards - provide a pixel classification, it has the advantage of giving directly the plots boundaries and an accurate estimation of the inter-row width and row orientation values. Another significant advantage is that good results are obtained with the red channel, present in widely available natural colors images. Moreover, since the appropriate spatial resolution is linked to the local pattern period, a coarser one could be used in many vine growing regions, especially dry ones (such as in Spain) where inter-row widths are up to 3 m. Then, panchromatic channels provided by satellites such as Ikonos or Quickbird could be used.

The main limit of this method is that it has to be applied on linear row patterns. It is not appropriate to detect level line vineyards such as encountered in certain vineyard regions with significant slopes (Portugal, Italy).

Some plans to apply this method in the future on very large areas (*i.e.* a complete DOC region of about one hundred thousand hectares) are presently under progress, as well as a detailed comparison with other published methods (such as the one presented in [13]).

ACKNOWLEDGMENT

The present study has been partly carried out within the European research project Bacchus (EVG2-2001-00023) with a co-funding from the European Commission. Aerial images were acquired by the *Avion Jaune* company (www.lavionjaune.com).

REFERENCES

[1] L. Garcin, X. Descombes, J. Zerubia, and L. M. H., "Building detection by Markov Object processes and a MCMC algorithm," INRIA, Tech. Rep. 4206, 2001.  
 [2] K. Segl, S. Roessner, U. Heiden, and H. Kaufmann, "Fusion of spectral and shape features for identification of urban surface cover types using reflective and thermal hyperspectral data," *ISPRS Journal of Photogrammetry and Remote Sensing*, vol. 58, pp. 99–112, 2003.  
 [3] V. Barbezat, P. Kreiss, A. Sulzmann, and J. Jacot, "Automated recognition of forest patterns using aerial photographs," in *SPIE: Optics in Agriculture, Forestry, and Biological Processing II, Bellingham (Washington)*, 1996.

[4] S. E. Franklin, R. J. Hall, L. M. Moskal, A. J. Maudie, and M. B. Lavigne, "Incorporating texture into classification of forest species composition from airborne multispectral images," *International Journal of Remote Sensing*, vol. 21, pp. 61–79, 2000.  
 [5] L. Moskal, "Investigating texture inversion in high-resolution multispectral imagery; implications for forest classification," in *Annual conference and FIG XXII Congress, Washington, D. C.*, 2002.  
 [6] W. Bobillet, J.-P. Da Costa, C. Germain, O. Laviaille, and G. Grenier, "Row detection in high resolution remote sensing images of vine fields," in *European Conference on Precision Agriculture*, J. Stafford and A. Werner, Eds. Berlin: Wageningen academic publishers, 2003, pp. 81–87.  
 [7] T. Wassenaar, J.-M. Robbez-Masson, P. Andrieux, and F. Baret, "Vineyard identification and description of spatial crop structure by per-field frequency analysis," *International Journal of Remote Sensing*, vol. 23, no. 17, pp. 3311–3325, 2002.  
 [8] A. Hall, J. Louis, and D. Lamb, "Characterising and mapping vineyard canopy using high-spatial-resolution aerial multispectral images," *Computers and Geosciences*, vol. 29, pp. 813–822, 2003.  
 [9] T. Ranchin, M. Albuissou, B. Naert, and G. Boyer, "The VINIDENT study: evaluation studies on the identification of vines using aerial photography in france." MARS Project, Contract 12606-97-02- FIED ISP F - Armines, Tech. Rep. TM/97/R/19, 1998.  
 [10] T. Ranchin, B. Naert, M. Albuissou, G. Boyer, and P. Astrand, "An automatic method for vine detection in airborne imagery using wavelet transform and multiresolution analysis," *Photogrammetric Engineering and Remote Sensing*, vol. 67, no. 1, pp. 91–98, Janvier 2001.  
 [11] T. A. Warner and K. Steinmaus, "Spatial classification of orchards and vineyards with high spatial resolution panchromatic imagery," *Photogrammetric Engineering and Remote Sensing*, vol. 71, no. 2, pp. 179–187, 2005.  
 [12] V. Muron and C. Jacquet, "Mise au point de méthodes pour le comptage des oliviers," *Société Française de Photogrammétrie et Télédétection*, vol. bulletin 164-165, pp. 87–95, 2001-2002.  
 [13] J.-P. Da Costa, F. Michelet, C. Germain, O. Laviaille, and G. Grenier, "Delineation of vine parcels by segmentation of high resolution remote sensed images," *Precision Agriculture*, vol. 8, no. 1, pp. 95–110, 2007.  
 [14] C. Delenne, S. Durrieu, G. Rabatel, M. Deshayes, J.-S. Bailly, C. Lelong, and P. Couteron, "Textural approaches for vineyard detection and characterization using very high spatial resolution remote-sensing data." *International Journal of Remote Sensing*, in press.  
 [15] C. Delenne, G. Rabatel, V. Agurto, and M. Deshayes, "Vine plot detection in aerial images using fourier analysis," in *1st International Conference on Object-based Image Analysis (OBIA 2006)*, S. Lang, T. Blaschke, and E. Schpfer, Eds., 2006.  
 [16] D. Gabor, "Theory of communication," *Journal of the Institution of Electrical Engineers*, vol. 93, no. 26, pp. 429–457, 1946.